METALLURGICAL INVESTIGATIONS ON ELECTRON BEAM WELDED DUPLEX STAINLESS STEELS

S. Krasnorutskyi, D. Keil, S. Schmigalla,
M. Zinke, A. Heyn and H. Pries

ABSTRACT

Thick-walled components made of duplex stainless steels are used in the semi-finished products as well as in machinery, apparatus and plant construction. Electron beam welding (EBW) of these components may be recommended for economic and quality reasons. To guarantee the necessary mechanical and technological properties and the corrosion resistance, the duplex stainless steels are welded with filler material and afterwards undergo a post-weld heat treatment. The present work shows interim results of investigations concerning the development of an electron beam multi-process technology for welding these steels without filler material and post-weld heat treatment. The studies were performed on standard duplex stainless steel of type 1.4462 (X2CrNiMoN22-5-3). When welding duplex stainless steels, the cooling rate and the chemical composition have a crucial influence on the final result. Based on fundamental investigations relating to the influence of the process parameters on the effusion of nitrogen and the cooling rates, the resulting austenite formation, mechanical properties and the corrosion resistance were taken into account to develop appropriate electron beam multi-process techniques. The ferrite content was measured metallographically and by magnetic induction, the impact toughness was measured at –40 °C and the determination of critical pitting temperatures was performed using electrochemical noise measurements.

IIW-Thesaurus keywords: Duplex stainless steels; EB-welding; Pitting corrosion; Microstructure; Fracture toughness; Nitrogen; Ferrite; Weld metal; Welding without filler.

1 Introduction

Duplex stainless steels are characterised by a two-phase austenite-ferrite microstructure which exhibits a combination of the properties of ferritic stainless steels and austenitic stainless steels. Optimum metallurgical and technological properties are achieved when the ferritic/austenitic microstructure consists of approximately 40-60 % ferrite [1]. In this case, such steels exhibit high strength, good pitting and crevice corrosion resistance and very good toughness values, even at low temperatures.

When the duplex stainless steels are electron beam (EB-) welded, matching chemical composition or higher alloyed chemical composition filler materials are used in the form of a preplaced nickel foil or wire in order to achieve the base material properties [2]. A better means of guaranteeing the weld seam properties is a subsequent solution heat treatment and water quenching, as specified in the pertinent standards for tubing production, for example, ASTM standards A 928, A 312 and A 358. According to [3], proportions of ferrite of up to 65 % are permissible for such weld seams. Higher values not only potentially reduce the impact toughness, but can lead to a greater susceptibility to hydrogen assisted cracking presuming an increasing hydrogen supply [4]. [5] also note that corrosion resistance may be reduced.

Current positive results from using EB-welding in the manufacture of longitudinal welded thick-walled pipes [6, 7] from duplex stainless steels has logically led to its expansion to other thick-walled components, such as centrifuge rotors, separators, etc., in other branches of industry. In such instances, avoiding expensive filler materials and costly post-weld heat treatment would be of considerable economic interest.

Conventional single-beam technology has yet to provide any economically feasible solutions for enabling the EB-welding of thick-walled duplex stainless steels without a filler metal or post-weld heat treatment as documented by the problems listed below.

Previous tests conducted by [8, 9, 10] involving single-beam EB-welding in a vacuum have shown that from a metallurgical perspective unacceptably strong ferritisation occurs in the weld metal (Figure 1) due to the process-related rapid heating and cooling and the vacuum-related effusion of nitrogen. As a result of the low ambient pressure in the vacuum chamber (10^{-3} mbar), Sievert's law causes a significant reduction in the nitrogen content of the weld metal. This reduces the δ-γ-transformation temperature [11] which, together with the high cooling rates of the EBW process, leads to unacceptably high proportions of ferrite in the weld metal of greater than 90 %.

Doc. IIW-2264, recommended for publication by Commission II "Arc Welding and Filler Metals."

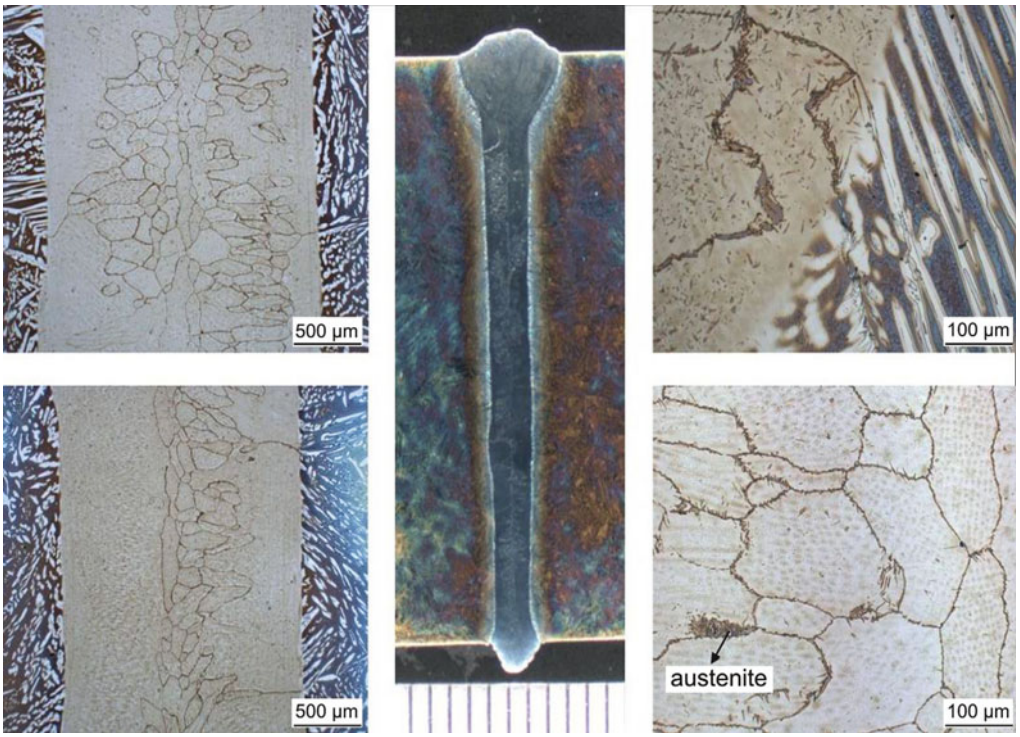

Figure 1 – Conventional single-beam EB-weld of a GX2CrNiMoN22-5-3 (1.4470) with a ferrite content of approximately 97 % in weld metal (measured via image analysis)

Nitrogen is also directly linked to the pitting corrosion resistance and the strength of the weld seam. This is mirrored in the Pitting Resistance Equivalent (PRE_N) among others.

$$PRE_N = \% Cr + 3.3 \times \% Mo + (16\text{-}30) \times \% N$$

A promising approach to electron beam welding thick-walled duplex stainless steels without a filler metal or post-weld heat treatment is provided by using the EB multi-process technologies developed in recent years. These technologies allow EB-welding to simultaneously generate multiple electron beams with different power distribution and focus position. This is realised by the quasi inertialess, high-frequency 3-dimensional deflection of the electron beam. The beam deflection is so quick that, for example, the vapour capillary remains intact while the beam is absent and does not collapse [12]. In addition to generating multiple weld pools, it is also possible to combine process stages such as preheating, welding and post-heating or smoothing of the seam. Thus, it is possible to considerably affect and optimise the thermal welding cycle.

2 Test material

This paper examines standard duplex stainless steel X2CrNiMoN22-5-3 (1.4462). The chemical composition and material properties are provided in Tables 1 and 2. The ferrite content of the base metal is measured by magnetic induction and via image analysis and amounts to approximately 55 FN or 48 % (Figure 2).

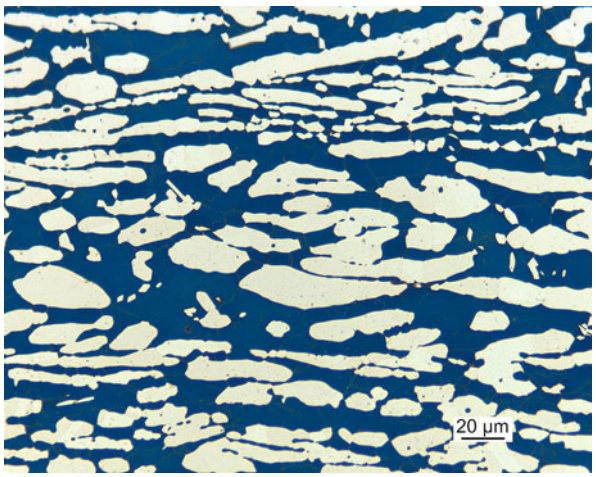

Figure 2 – Base metal microstructure of X2CrNiMo22-5-3; Etchant: Beraha II (austenite: white)

3 Experimental

To develop a multi-process technology for the quality assured manufacture of weld seams without using filler metal and/or subsequent heat treatment, it was first necessary to determine the cooling times (time between 1200 °C and 800 °C ($\Delta t_{12/8}$)) for guaranteeing the necessary mechanical and technological quality requirements and corrosion resistance.

For this reason, bead on plate welding was used on 16 mm-thick plates of 1.4462 with the specification that the seams had the minimum width of 5 mm technologically required

Table 1 – Mechanical properties of the test material

Material	s [mm]	R_m [MPa]	$R_{p0,2}$ [MPa]	A_5 [%]	$KV_{trans.}$ (–40 °C) [J]
1.4462 [13]	≤ 20	680-880	480	25	40
1.4462 (test certificate)	16.8	774	535	35	261

Table 2 – Chemical composition (wt.-%) of the test material

Material	C	Si	Mn	P	S	Cr	Ni	Mo	N	Fe
1.4462 [14]	≤ 0.030	≤ 1.00	≤ 2.00	≤ 0.035	≤ 0.015	21.00 - 23.00	4.50 - 6.50	2.50 - 3.50	0.10 - 0.22	Bal.
1.4462 (test certificate)	0.018	0.56	1.40	0.022	0.001	22.4	5.66	3.10	0.19	Bal.

for butt-welding and that their internal seam irregularities met quality level B (as per DIN EN ISO 13919-1 [15]). The occurrence of extreme geometric irregularities in the weld cap and weld root was tolerated, however. An electron beam welding facility with an acceleration voltage of 150 kV, a maximum output of 15 kW and an operating pressure of 10^{-3} mbar was used to conduct the tests. The pressure in the electron gun was 10^{-5} mbar.

The cooling times were varied with respect to the use of the multiple-beam technique with repeated drive over (1-6 drive overs) and the associated preheating caused by the process heat (Table 3). All welds (drive overs) were carried out as full penetration welds with constant welding parameters. Additionally, the specimens were preheated before the first drive over with a defocused beam up to 400 °C. The time between two drive overs was app. 25 s. Such welding enabled a correlation between the proportions of ferrite, nitrogen content and mechanical and technological properties of the weld metals resulting from the various cooling times.

The cooling curves were recorded using 0.3 mm thick NiCr-Ni-thermocouples (Type K) which were resistance spot welded on the surface of the base metal. As the heat affected zone of an EB-weld is very narrow, the distance between the thermocouples and the fusion line was less than 1 mm.

Due to the narrow width of the bead on the plate, the proportion of ferrite was metallographically determined along the seam cross section. Mean values of the approximately 10 measurements each in the upper, middle and lower seam areas were calculated and compared.

The nitrogen content was measured by taking melt-extraction samples from the pure EB-weld metal.

The impact toughness at –40 °C was served as mechanical and technological quality parameter. It was determined by using Charpy VWT-specimens from the centre of the weld seam with a notched area perpendicular to the surface. This test temperature represents the lower service temperature of the duplex qualities, whereby the testing of the impact toughness at this temperature is required by various certification bodies. The MMA-welded samples listed in Table 4 were tested analogously as reference values.

The critical pitting temperature (CPT) was used to evaluate the pitting corrosion resistance of the weld metals and was determined by analysing the electrochemical noise (ECN) during the dynamic tempering of the test solution. The used measurement parameter was the current noise (IECN) between two identical specimens resulting from local dissolution of one of the two samples. Integrating the IECN values over the sample rate

Table 3 – Welding parameters for electron beam welding

No.	BM	FM	s [mm]	preheating [°C]	U [kV]	I [mA]	v [m/min]	$\Delta t_{12/8}$ [s]	note
EB-1	1.4462	-	16.8	395	150	42	0.5	4.5	1 drive over
EB-2	1.4462	-	16.8	340	150	43	0.5	7.4	2 drive overs
EB-3	1.4462	-	16.8	435	150	40	0.5	17.7	3 drive overs
EB-4	1.4462	-	16.8	370	150	35	0.5	30.3	4 drive overs
EB-5	1.4462	-	16.8	370	150	35	0.5	46.6	5 drive overs
EB-6	1.4462	-	16.8	370	150	34	0.5	48.7	6 drive overs

periods generated the characteristic load curves over the temperature profile. Compared to standard testing as per ASTM G48, this method has the advantage of being more objective when evaluating the load curves than the purely visual evaluations of the standard test procedure. Moreover, dynamic tempering means that the time and material intensive iterative method can be omitted. [16, 17]

Figure 3 (right) provides an example of the resulting charge-temperature curve and the linear regression that is used to determine the critical pitting temperatures.

A 6 % $FeCl_3$ solution as per ASTM G48-A was used for the test solution. Three specimens were taken from the upper area of each weld seam. The specimens were grinded on all sides (180 grit), pickled (30 min with Antox-pickling paste) and passivated (24 h desiccator at 84 % relative humidity). The CPT_{theor} was determined as a theoretical reference value using the formula as given in ASTM G48:

$$CPT_{theor}\,[°C] = 2.5 \times \%\,Cr + 7.6 \times \%\,Mo + 31.9 \times \%\,N - 41$$

4 Results and discussion

Having optimised the welding parameters, it was possible to create seams according to the requirements listed above.

The determined $\Delta t_{12/8}$-times could be controlled by repeated drive over the seams within a range of between 4 s and 50 s (cf. Table 3). In the case of 6-time drive over a short-term preheating of approximately 850 °C was achieved in the narrow weld zone. Due to the preheating the $\Delta t_{12/8}$ increased significant.

The short cooling times of 4.5 s (EB-1) and 7.4 s (EB-2) caused an unfavourable austenite-ferrite ratio in the primary ferritic solidifying weld metals (Figure 4). This is due to the suppression of the diffusion-controlled transformation of the ferrite into austenite. Thus, only small proportions of grain boundary austenite allotriomorphs are formed in the weld metal (Figure 4). The ferrite content in these EB-weld metals were 86 % or 82 % (mean values).

The best results in the series of tests with respect to the austenite-ferrite ratio were exhibited by the EB-weld with

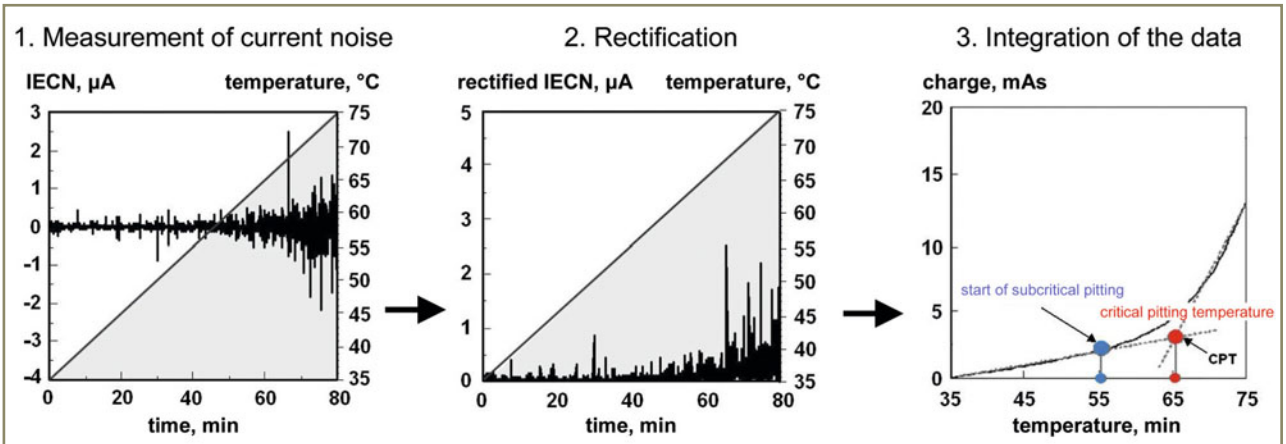

Figure 3 – General procedure for the evaluation of the electrochemical noise measurements [15]

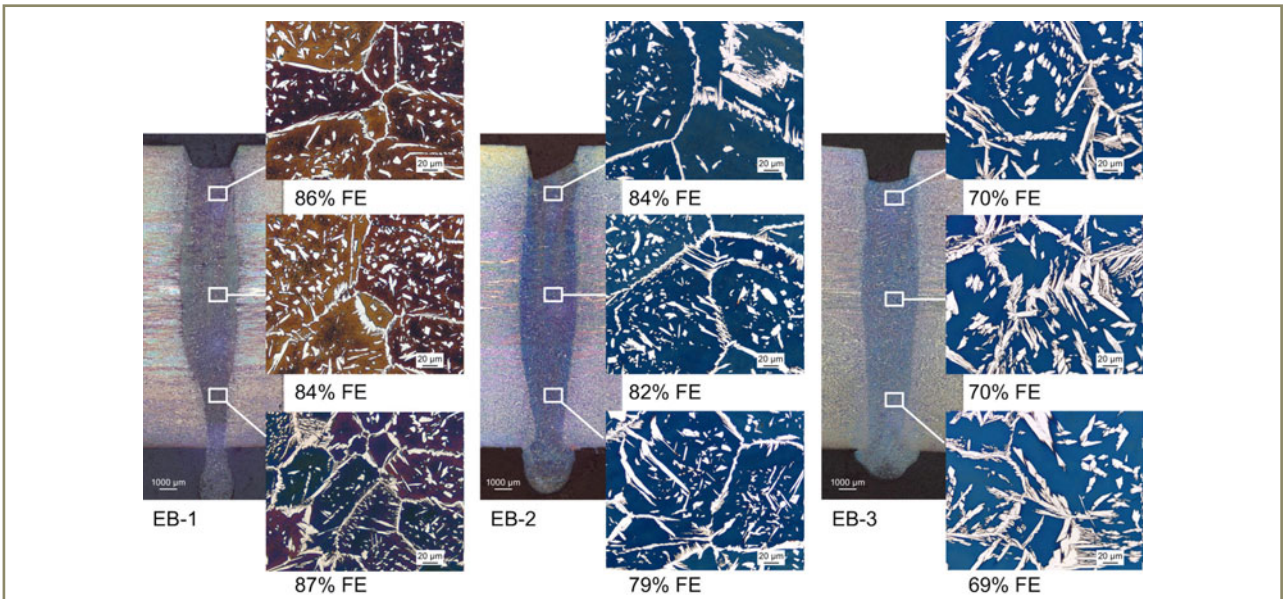

Figure 4 – Weld cross-section and the microstructure of the EB-welds EB-1, EB-2 and EB-3; Etchant: Beraha II (austenite: white)

a $\Delta t_{12/8}$-time of 17.7 s (EB-3). This one only consisted of 70 % ferrite and an even precipitation of austenite was evident in a partially Widmanstätten structure (Figure 4).

Despite the clearly higher $\Delta t_{12/8}$-times, the weld seams created by 4 to 6 drive overs once again exhibited an increase in the ferrite content of more than 80 %. This fact may be further explained by measuring the nitrogen content of the weld metal. The melt-extraction analysis of the nitrogen content of the generated weld metals indicated a clear reduction in nitrogen as the number of drive overs increased (Figure 5). With six drive overs, the nitrogen content of the weld metal was only 0.06 %, which equates to a threefold reduction in nitrogen compared to the base material. This explains the increase in the proportion of ferrite in the weld with 4 to 6 drive overs despite the longer cooling period.

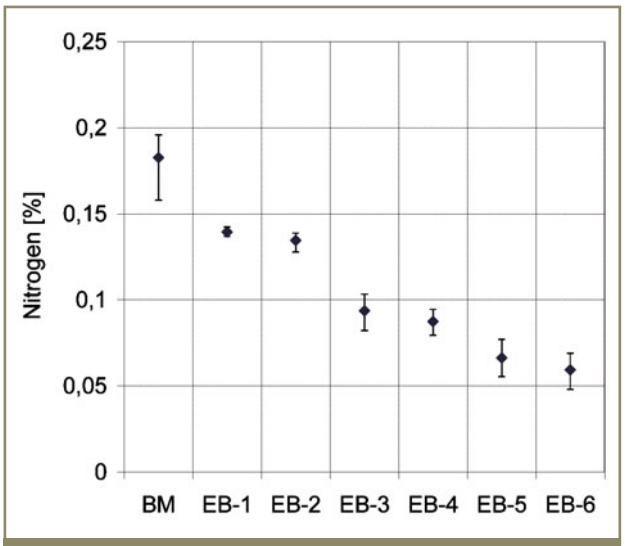

Figure 5 – Nitrogen content of the electron beam welds compared to that of base metal (1.4462)

For these welds, significant greater cooling times would be needed to achieve lower proportions of ferrite. Figure 6 clearly illustrates that weld EB-3 exhibited the most favourable austenite-ferrite ratio in the series of tests with a sufficiently long cooling time and a sufficiently high nitrogen content in the weld metal.

Impact toughness was determined using the EB-weld with the highest cooling rate (EB-1), the EB-weld with the most favourable austenite-ferrite ratio (EB-3), the base metal and the MMA-weld listed in Table 4.

As expected, weld EB-1 exhibited the poorest results due to the high ferrite content. EB-3 and the MMA-welds

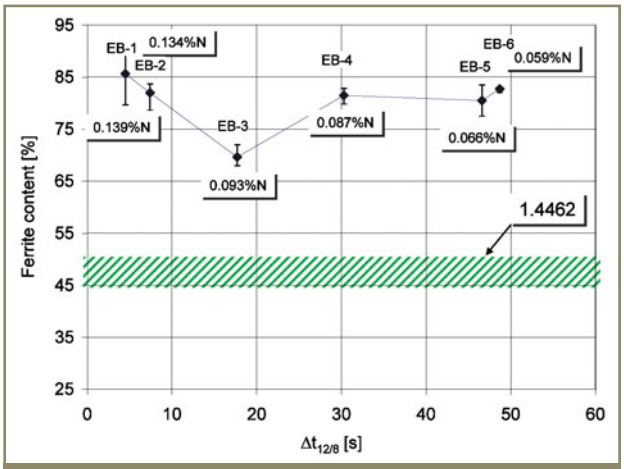

Figure 6 – Combination of ferrite content and nitrogen content in relation to $\Delta t_{12/8}$-time

both achieved comparable values of approximately 40 J (Figure 7). This is an acceptable result as this value is sufficient for a number of applications. For example, it complies with the impact toughness for 1.4462 of 40 J at a test temperature of -40 °C as specified by VdTÜV Material Sheet 418 [13].

The preheating temperatures within the test series clearly exceeded the recommended preheating and service temperatures of the base metal, even if it is just for a short-term [13]. According to [18] a variety of undesirable secondary phases can form when welding duplex stainless steels and exceeding the time in the critical temperature range. Due to this fact, every specimen was examined metallographically and by hardness measurements. As expected, the results showed no formation of undesirable secondary phases in the weld zone.

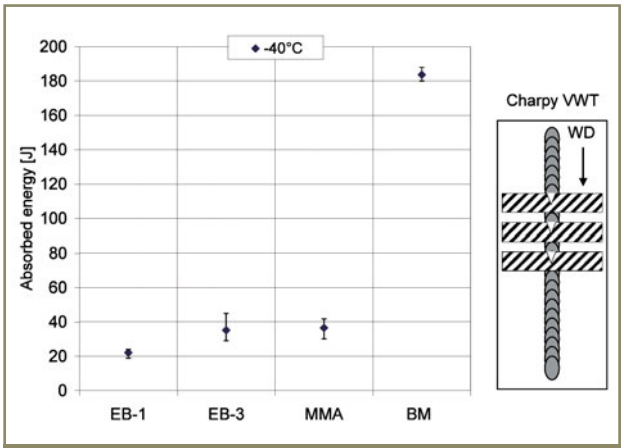

Figure 7 – Impact toughness of weld and base metal at -40°C (Charpy VWT)

Table 4 – Welding parameters for MMA-welding

No.	BM	FM	s [mm]	preheating [°C]	U [V]	I [A]	v [m/min]	$\Delta t_{12/8}$ [s]	note
MMA	1.4462	E 22 9 3 N L R 32 (AROSTA 4462)	16.8	100-120	-	160-210	-	-	8 layers

The analysis of the corrosion specimens clearly shows that pitting corrosion is obviously associated with the weld metal (Figure 8). This can be identified in all the analysed specimens. Table 5 compares the results determined by ECN of the CPT of the base metal and EB-welded specimens with 1, 3 and 6 drive overs (EB-1, EB-3, EB-6) in relation to the nitrogen content of the weld metals.

These series of tests clearly illustrate the effect of nitrogen on the CPT. However, as it was already expected from the calculated values CPT_{theor}, the decrease in the CPT is low and does not affect the possible applications of the weld joint.

5 Summary and outlook

The initial results show that it is possible to increase the $t_{12/8}$ time significantly due to repeated remelting of the weld seams by multiple drive over of the electron beam. However, with increasing number of drive overs, a significant loss of nitrogen content in the weld metal was observed. Despite longer cooling times a further reduction of ferrite content in the weld seams was not possible. The current results show that with 70 % ferrite and 0.093 % nitrogen, three is the optimum number of drive overs. The weld with three drive overs achieved impact toughness values comparable to those of MMA-welds with the same type of filler metal.

The investigation to determine the corrosion behaviour using electrochemical noise measurements revealed a significant influence of nitrogen on the critical pitting temperature. Due to the nitrogen degassing during welding a drop of the critical pitting temperature was observed. As expected the critical pitting temperature is only slightly lower than that of the base metal, which does not affect the field of application of the weld joint.

Within the next investigations a transfer of the results to the multi-beam technique will be performed with the aim of further reduction the ferrite content in the weld metal and to guarantee high process reliability.

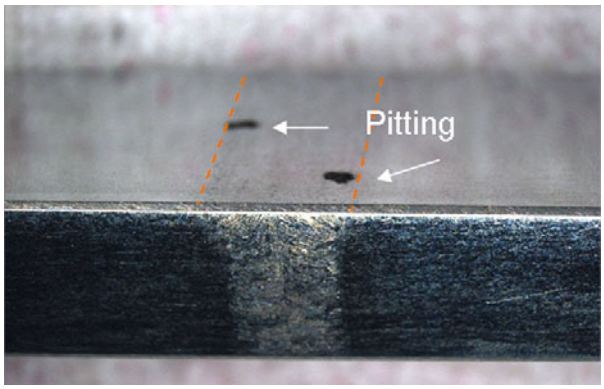

Figure 8 – Photograph of an ECN-specimen with pitting corrosion in weld metal

Acknowledgement

These tests were funded by the Federal Ministry of Economics and Technology (BMWi) assisted by the Arbeitsgemeinschaft industrieller Forschungsvereinigungen (AiF - industrial research consortium) “Otto von Guericke” e.V. (AiF-No. 16.277 B/DVS-Nr. 1.066) and supported by the DVS Forschungsvereinigung Schweißen und verwandte Verfahren e. V. (DVS institute for welding and related processes). The authors gratefully acknowledge the support.

References

[1] Gunn R. N.: Duplex stainless steels. Microstructure, properties and applications. Cambridge 1997.

[2] Hoffmann R., Schüller T. and Sölch R.: Electron beam welding of duplex stainless steel with filler material in form of preplaced foils, Elektronenstrahlschweißen eines Duplexstahls mit bandförmigem Zusatzwerkstoff, Schweißen und Schneiden, 2001, no. 3, pp. 148-155 (in German).

[3] Shell: Duplex and superduplex stainless steel pipe. Amendments/supplements to ASTM A 928, 2007.

[4] Gooch T. G., Leonard A. J.: Hydrogen cracking of ferritic-austenitic stainless steel weld metal: Duplex America 2000, Conference on duplex stainless steels: conference papers. Zutphen op. 2000, pp. 345-357.

[5] Lefebvre J.: Guidance on Specifications of Ferrite in Stainless Steel Weld Metal, Doc. IIW-1166, Welding in the World, 1993, vol. 31, no. 6, pp. 390-407.

Table 5 – Results of the electrochemical noise measurements in relation to the welding parameters/nitrogen content

	BM	EB-1	EB-3	EB-6
Nitrogen [%]	0.183	0.139	0.093	0.059
Ferrite [%]	48	86	70	83
$CPT_{theor.}$ [°C]	45.2	43.7	42.3	41.2
CPT_{exper} [°C]	50.5	44.6	43.2	41.4
Occurrence	BM	WM	WM	WM

[6] Sölch R.: The production of thickwalled longitudinally welded pipes made of stainless steel, Herstellung längsnahtgeschweißter Edelstahlrohre mit größerer Wanddicke: Schweißen und Schneiden 2001. Vorträge der gleichnamigen Großen Schweißtechnischen Tagung in Essen vom 11. bis 13. September. Düsseldorf 2001, pp. 121-128. (in German)

[7] Sölch R.: Electron beam welding for production of longitudinally welded pipes, Elektronenstrahlschweißen beim Herstellen von längsnahtgeschweißten Rohren: Schweißen und Schneiden 2004. Vorträge der gleichnamigen Großen Schweißtechnischen Tagung in Magdeburg vom 22. bis 24. September 2004. Düsseldorf 2004, pp. 104-109 (in German).

[8] Steffens H. D., Hartung F. and Buchmann C.: Electron beam welding of duplex stainless steel X2CrNiMoN2253, Elektronenstrahlschweißen des Duplexstahls X2CrNiMo N2253: Schweißen und Schneiden '93, Vorträge der gleichnamigen Großen Schweißtechnischen Tagung in Essen vom 15. bis 17. September 1993. Düsseldorf 1993, pp. 81-85 (in German).

[9] Cvijovic Z., Knezevic V., Mihaijovic D. and Radenkovic G.: Effect of welding process on the microstructure of duplex stainless steel: Welding Science and Technology, Japan-Slovak Welding Symposium 1996, pp. 109-114.

[10] Muthupandi V., Balasrinivasan P., Seshadri S. and Sundaresan S.: Effect of weld metal chemistry and heat input on the structure and properties of duplex stainless steel welds, Materials Science and Engineering A, 2003, vol. 358, no. 1-2, pp. 9-16.

[11] Mundt R. and Hoffmeister H.: Effect of chemical composition and weld thermal cycles on phase transformation and microstructures of ferritic-austenitic steels: Stainless Steels '84. Proceedings of the conference, Göteborg, on 3 - 4 September 1984. London 1985, pp. 315-322.

[12] Dobeneck D. von, Löwer T. and Adam V.: Electron beam welding. The process and its industrial applications for highest productivity. Elektronenstrahlschweißen. Das Verfahren und seine industrielle Anwendung für höchste Produktivität. Landsberg/Lech 2001 (in German).

[13] VdTÜV- Material Data Sheet 418: ferritic – austenitic rolled and forged stainless steel, X2CrNiMoN 22-5-3, material number 1.4462, VdTÜV-Werkstoffblatt 418: Ferritisch-austenitischer Walz- und Schmiedestahl, X2CrNiMoN 22-5-3, Werkstoff-Nr. 1.4462, Ausgabe 12.20[14] DIN EN 10088-3:2005, Stainless steels – Part 3: Technical delivery conditions for semi-finished products, bars, rods, wire, sections and bright products of corrosion resisting steels for general purposes; German version EN 10088-3:2005.

[15] DIN EN ISO 13919-1, Welding – Electrons and laser beam welded joints; guidance on quality levels for imperfections - Part 1: Steel (ISO 13919-1:1996).

[16] Göllner J., Burkert A. and Heyn A.: Electrochemical noise measurements – Innovation in corrosion testing, Elektrochemische Rauschmessungen – Innovation in der Korrosionsprüfung, Materials and Corrosion, 2002, vol. 53, no. 9, pp. 656-662 (in German).

[17] Heyn A. and Göllner J.: Using electrochemical noise for corrosion testing: Determination of critical pitting temperatures. Materials and Corrosion, 2007, vol. 58, no. 12, pp. 953-960.

[18] Karlsson L., Rigdal S. and Lake F.: Effects of intermetallic phases in duplex stainless steel weldments – A critical review: Duplex America 2000. Conference on duplex stainless steels: conference papers. Zutphen op. 2000, pp. 257 272.

About the authors

Sergii Krasnorutskyi, Sven Schmigalla, Manuela Zinke and Andreas Heyn are with the Institute of Materials and Joining Technology, Otto von Guericke University of Magdeburg, Germany. Helge Pries is with the Institute of Joining and Welding, Braunschweig University of Technology, Germany. Daniel Keil (daniel.keil@volkswagen.de) formerly with Institute of Materials and Joining Technology, Otto von Guericke University of Magdeburg, is now with Volkswagen AG, Wolfsburg (Germany).